Communication

# Collapse in Crystalline Structure and Decline in Catalytic Activity of Pt Nanoparticles on Reducing Particle Size to 1 nm

Yubao Sun, Lin Zhuang, Juntao Lu, Xinlin Hong, and Peifang Liu

*J. Am. Chem. Soc.*, **2007**, 129 (50), 15465-15467 • DOI: 10.1021/ja076177b



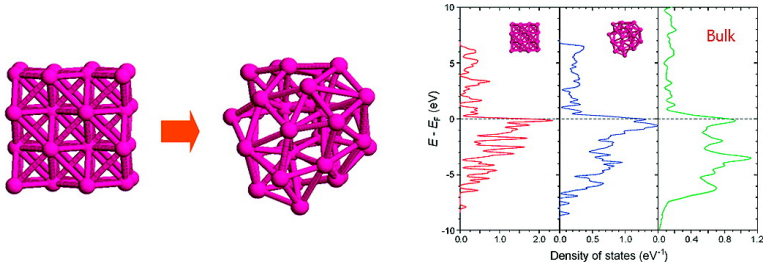


## More About This Article

Additional resources and features associated with this article are available within the HTML version:

- Supporting Information
- Links to the 6 articles that cite this article, as of the time of this article download
- Access to high resolution figures
- Links to articles and content related to this article
- Copyright permission to reproduce figures and/or text from this article

View the Full Text HTML

J|A|C|S
COMMUNICATIONS

Published on Web 11/22/2007

# Collapse in Crystalline Structure and Decline in Catalytic Activity of Pt Nanoparticles on Reducing Particle Size to 1 nm

Yubao Sun, Lin Zhuang,* Juntao Lu, Xinlin Hong, and Peifang Liu

*Department of Chemistry, Wuhan University, Wuhan 430072, China*

Received August 16, 2007; E-mail: lzhuang@whu.edu.cn

Combined experimental and computational studies show that, upon reducing the diameter of Pt nanoparticles down to 1 nm, a collapse in the crystalline structure occurs spontaneously and the thus-induced quantum size effect causes a decline in the catalytic activity toward $H_2$ electrooxidation. Platinum has been playing a vital role in heterogeneous catalysis, especially for low-temperature fuel cells. To maximize Pt utilization, nanoparticles are usually applied, with the particle size expected to be as small as possible. However, the particle-size dependent catalytic activity of Pt, determined by the interplay of surface geometric and electronic factors, is not quite straightforward in the range of a few nanometers.[1−4] For $CO_{ads}$ oxidation,[1] methanol oxidation,[2] or oxygen reduction,[3] the catalytic activity of Pt nanoparticles was found, by most studies, to decrease on reducing the particle size, and the maximum mass-specific activity (MSA) was estimated to appear at around 3 nm.[2b,3d] For hydrogen oxidation reaction (HOR), the situation seems rather different; the catalytic activity of Pt nanoparticles was found to be almost unchanged or even increasing upon reducing the particle size.[4] Thus it is still suspected whether the Pt utilization for fuel cell hydrogen anodes can be further increased by reducing the Pt particle size down to 1 nm or even smaller.

To explore the possible lower size limit of Pt as a HOR catalyst and to reveal the underlying science is not only a yet unresolved topic of great concern for fuel cell developers but also a general subject of fundamental and technological significance. In the present work, we report a successful preparation of ultrafine Pt/C catalysts with the Pt particle size reduced to about 1 nm, and the resulting changes in the crystalline structure, electronic structure, and catalytic activity toward HOR.

The ultrafine Pt nanoparticles were synthesized using the improved impregnation method reported in our previous work[5a] and by employing mesoporous carbon black CMK-3 as the catalyst support, which was produced according to the well-documented template method.[5b,c] The BET-specific surface area of CMK-3 is about 1200 $m^2/g$, almost five times of that of XC-72, the most frequently used carbon support for fuel cell catalysts. It turned out that such a high specific surface area greatly enhanced the dispersion of Pt nanoparticles. As shown in Figure 1a, Pt/XC-72, synthesized by the same procedure, shows a clear Pt face-centered cubic (fcc) structure in its X-ray diffraction (XRD) pattern, with a particle size estimated from the line width to be 2.5 nm; whereas Pt/CMK-3 totally loses the crystalline feature in its XRD spectrum, indicating that the Pt particles dispersed on CMK-3 should be extremely small and/or in a noncrystalline state.

Figure 1b shows a representative high-resolution transition electron microscopy (HRTEM) image of Pt particles dispersed on CMK-3. In the center of this image, a dark spot, without any crystalline pattern, can be well distinguished from the graphited carbon background and estimated to be around 1 nm in diameter.

The lack of crystalline pattern in the particle image is not due to the resolution limitation of the microscope (JEOL JEM-2010FEF, with an ultimate spatial resolution of 0.19 nm) but rather reflects the amorphous nature of the Pt particles. In some locations of the same sample, a few bigger particles (greater than 1.5 nm in diameter) with clear crystalline pattern can be observed (Figure 1c).

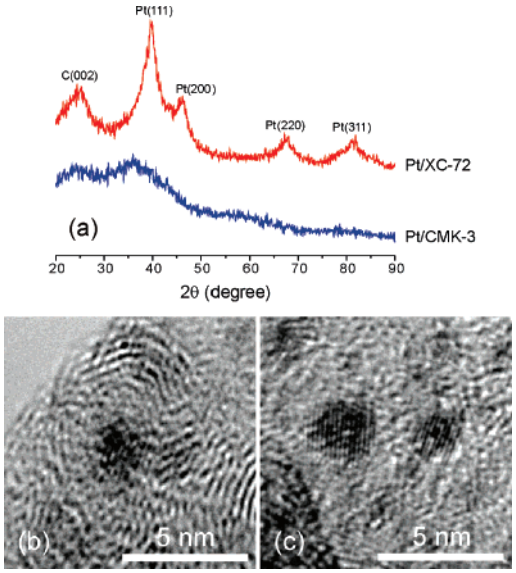


***Figure 1.*** (a) XRD patterns of Pt/XC-72 and Pt/CMK-3. Pt loadings in both catalysts are 20 wt %. (b) A representative HRTEM image of the Pt particles dispersed on CMK-3. (c) HRTEM images of crystalline Pt particles rarely found in Pt/CMK-3.

It can be concluded from the HRTEM observation that most Pt particles in Pt/CMK-3 are around 1 nm in diameter and, more importantly, in an amorphous structure. Such noncrystalline Pt particles are very unusual and, therefore, need further confirmation. An alternative explanation of the noncrystalline spots seen in the HRTEM image might be Pt compounds, such as Pt precursors, instead of metallic Pt. To ascertain the metallic nature of the platinum in the sample, X-ray photoelectron (XPS) examinations have been conducted to compare the oxidation state of Pt in the catalyst before and after the $H_2$ reduction procedure in the preparation. As revealed by the results in Figure S1 and Table 1, it is evident that metallic Pt was formed after $H_2$ reduction. Note that there were also PtO and $PtO_2$ components after $H_2$ reduction, but they should be ascribed to the surface oxidation of Pt nanoparticles on exposure to air.

An especially fundamental question is whether the formation of noncrystalline Pt nanoparticles is a natural consequence of reducing the particle size down to 1 nm. To unveil the atomic packing behavior in a Pt nanoparticle as a function of the particle size, molecular dynamic (MD) simulations were carried out using the semiempirical effective medium theory developed by Nørskov and co-workers,[7a] which has been proven to be accurate in describing structural and thermal properties of fcc metals.[7]

***Table 1.*** XPS Results for Pt/CMK-3 before and after $H_2$ Reduction, Deduced from the Curve Fitting in Figure S1

| signal/sample | binding energy (eV) | reference BE (eV)[6] | suggested formula[6] | atomic ratio (%) |
|---|---|---|---|---|
| Pt $4f_{7/2}$ (before $H_2$ redn) | 72.2 | 72.4 | $PtCl_2$, PtO | 56.6 |
| | 73.9 | 74.2 | $PtCl_4$, $PtO_2$ | 43.4 |
| Pt $4f_{7/2}$ (after $H_2$ redn) | 71.5 | 70.8 | Pt | 36.4 |
| | 72.8 | 72.4 | PtO | 36.0 |
| | 74.5 | 74.2 | $PtO_2$ | 27.6 |

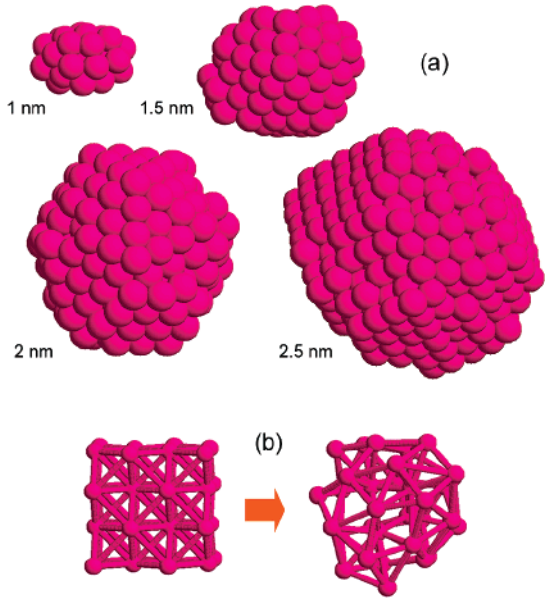


***Figure 2.*** Molecular dynamic simulations using the effective medium theory.[7a] (a) Four Pt cubic particles with different diameters, defined in this work as the diameter of a sphere with a volume equal to the cubic, were heated in vacuum to 2000 K (Figure S2) and then slowly cooled down to 300 K, resulting in different atom-packing structures as a function of the particle size. (b) A virtual Pt cubic particle of 1 nm diameter was thermostatically kept at 300 K in vacuum for a period of time, a spontaneous collapse in the crystalline structure occurring quickly.

The MD simulation was started by constructing an ordered Pt fcc cube with a given diameter and heating to 2000 K in vacuum to obtain a disordered assembly of Pt atoms (Figure S2), which was then followed by an annealing process (slowly cooling down to 300 K). What we are interested in is whether an ordered structure will result upon annealing. Four Pt cubic particles with different diameters (1, 1.5, 2, and 2.5 nm, defined in this work as the diameter of a sphere with a volume equal to the cubic) were tested by the MD simulation, and the structures obtained after annealing are shown in Figure 2a. It is clear that for relatively big particles, such as the one of 2.5 nm diameter, ordered structure can be spontaneously established during the annealing process, with well-defined fcc (100) and fcc (111) facets exposed on the surface. On reducing the particle diameter, the size of fcc (100) and fcc (111) facets decreases and more kink structures appear on the surface. For the particle of 1 nm diameter, no ordered surface resulted at all. This MD simulation clearly demonstrates that the formation of amorphous structure is inevitable for Pt nanoparticles on reducing the diameter down to 1 nm.

Another relevant MD simulation was conducted to examine the structural stability of a Pt nanocrystal at room temperature. A virtual Pt cubic particle of 1 nm diameter with regular fcc structure was thermostatically kept at 300 K in vacuum for a period of time (50 ps). As illustrated in Figure 2b, the crystalline structure was found to collapse quickly to a disordered structure, with a contraction in the particle volume by about 10%. Such a structural collapse did not occur to a Pt nanocrystal of 2.5 nm diameter; the thermal motion of atoms at room temperature only lead to a "truncation" on the sharp corners of the Pt cube (Figure S3), with the bulk structure essentially unchanged. This MD simulation indicates that, when the particle diameter reduced to 1 nm, crystalline structure is unstable even at room temperature and the formation of a noncrystalline structure is spontaneous. The shrink in particle volume should be attributed to the surface tension which causes a converging pressure inversely proportional to particle diameter.

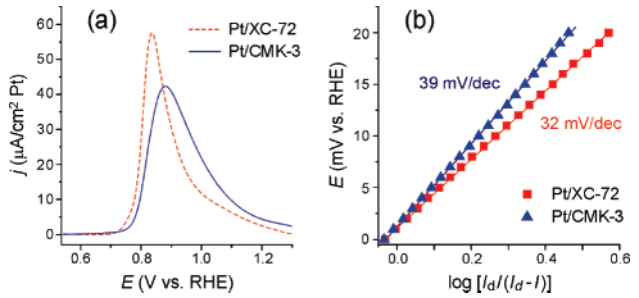


***Figure 3.*** (a) CO stripping profiles for Pt/XC-72 and Pt/CMK-3, obtained by differentiating the $I-V$ curves of Pt in 0.5 M $H_2SO_4$ solution with and without CO (Figure S4). (b) $E$ vs $\log[I_d/(I_d - I)]$ plots for HOR on Pt/XC-72 and Pt/CMK-3, where $I_d$ is the diffusion limiting current.

Now that amorphous 1 nm Pt nanoparticles have been theoretically confirmed to be feasible and experimentally obtained, it will be interesting to see how the structural peculiarity influences their catalytic activity, especially toward HOR. Before comparing the activity between Pt/CMK-3 and Pt/XC-72 for HOR, CO stripping experiments were carried out to characterize the surface (see the Supporting Information for experimental details). Figure 3a presents the CO stripping profiles of Pt/XC-72 and Pt/CMK-3, which were obtained by differentiating the $I-V$ curves of Pt in $H_2SO_4$ solution with and without CO (Figure S4). A positive shift in the peak potential is evident for Pt/CMK-3 compared to Pt/XC-72, indicating that CO adsorption is stronger on Pt/CMK-3 than on Pt/XC-72, which is in agreement with the reported trend that CO adsorption is stronger on smaller Pt nanoparticles.[1] Also, the peak of CO stripping on Pt/CMK-3 is wider than that on Pt/XC-72, implying slower kinetics and/or the surface nonuniformity because of disordered structure.

HOR was investigated using a rotating glassy-carbon electrode on which Pt/C catalysts were loaded. As shown in Figure 3b, at low overpotentials, the potential−current relationship for HOR on both Pt/XC-72 and Pt/CMK-3 correspond to a linear correlation of $E$ vs $\log[I_d/(I_d - I)]$ rather than a Tafel linearity (Figure S5). Such behavior can be ascribed to the fast kinetics of HOR through a Tafel-Volmer mechanism:[4a,8]

$$H_2 + 2Pt \leftrightarrow 2Pt{-}H_{ads} \quad \text{(Tafel reaction)}$$

$$Pt{-}H_{ads} \leftrightarrow Pt + H^+ + e^- \quad \text{(Volmer reaction)}$$

The slope of the $E$ vs $\log[I_d/(I_d - I)]$ linearity for Pt/XC-72 is 32 mV/dec, the same as reported in the literature[4a] and slightly higher than the theoretical value of 29.6 mV/dec (corresponding to a reversible two-electron reaction); while for Pt/CMK-3, the slope increases to 39 mV/dec, indicating a decrease in the reversibility of the electrode reaction.

To evaluate the change in the catalytic activity, the exchange current density ($j_0$) of the hydrogen reaction is calculated using the equation proposed by Chen and Kucernak (Supporting Information, eq S1),[8] and normalized to the electrochemical surface area

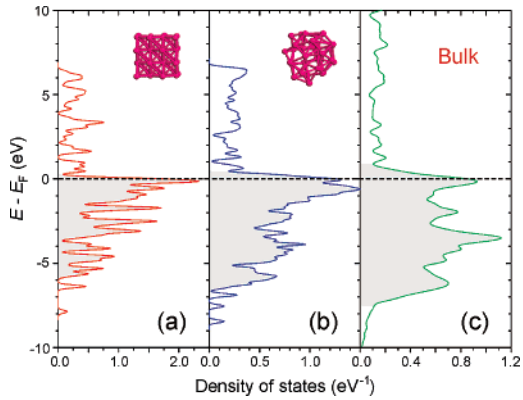


***Figure 4.*** Band structures, obtained from DFT calculations, for (a) a virtual Pt cubic particle of 1 nm diameter with regular fcc structure, (b) a Pt nanoparticle of 1 nm diameter with amorphous structure deduced from the MD simulation illustrated by Figure 2b, and (c) bulk Pt metal. DOS is normalized to a single Pt atom. The shadowed parts indicate the d bands.

determined by the CO stripping charge. The $j_0$ for Pt/XC-72 thus obtained is 0.16 mA/cm$^2$, the same as that reported in the literature for the same type of catalyst,[4a] whereas the $j_0$ for Pt/CMK-3 is 0.068 mA/cm$^2$, showing a remarkable decline in the catalytic activity for HOR.

Such a decline in activity should stem from the special electronic nature of the amorphous structure. To unravel the physical essence of the electronic effect, density functional theory (DFT) was employed to calculate the band structure for Pt nanoparticles of 1 nm diameter. Two particle structures, corresponding to the beginning and the end state of the room-temperature MD simulation illustrated in Figure 2b, have been calculated, and the results are shown in Figure 4a and 4b, respectively, along with the band structure of bulk Pt metal (Figure 4c) for comparison.

For the virtual crystalline 1 nm Pt particle, because of the limited number of atoms (only 32 atoms in a particle), the molecular orbitals are relatively separated and localized (Figure 4a), in contrast to the continuous and extending valence band (hybrid d band and sp band) for bulk Pt metal (Figure 4c). At the same time, the band widths of both the d band and sp band are significantly smaller than those of bulk Pt metal, as expected.

It is interesting to see the change in the band structure upon relaxing the 1 nm Pt nanocrystal to the amorphous state. As shown in Figure 4b, because of the above-mentioned volume contraction (decrease in the Pt−Pt distance), the enhanced overlap of atomic orbitals results in a merging of neighboring bands in Figure 4a to form a special band structure, the feature of which appears, interestingly and somewhat unexpectedly, in between Figure 4a and 4c. The d band of the amorphous Pt ultrafine particle is much narrower than that of bulk Pt metal, resulting in an increase in the density of states at the Fermi level, DOS($E_F$), and an upward shift in the d band center with respect to $E_F$. Such electronic characteristics would lead to an enhancement in the interaction between the surface and the adsorbates,[9] which is in line with the CO stripping experiment.

On Pt/CMK-3, the Pt−$H_{ads}$ bond is thus expected to be stronger than on Pt/XC-72. On one hand, this would be favorable to the Tafel reaction; but on the other hand, it could inhibit the Volmer reaction and decrease the turnover frequency correspondingly. Unfortunately, it seems that the negative impact is greater in this case.

Such a quantum size effect would occur only when the particle size is sufficiently small (1 nm in this case), and is fundamentally different from the particle size effect observed in the range of a few nanometers,[1−4] in which the variation of adsorption sites (crystalline facet, defect) is believed to be crucial while the electronic properties do not differ much from those of the bulk metal.[10]

In a practical standpoint, despite a big loss in the surface-specific activity, the MSA of Pt/CMK-3 toward HOR can still be roughly equal to that of Pt/XC-72. But 1 nm should be considered to be the lower size limit for Pt as a HOR catalyst; further decrease in particle size will cause a decline in MSA.

Not only has the present work estimated the Pt utilization limit for HOR, but it also expands the structure−activity relationship of Pt nanoparticles toward HOR to an extent that has rarely been touched, which provides valuable mechanistic insights into the catalyst design for fuel cells and alike heterogeneous catalytic processes.

**Acknowledgment.** This work was financially supported under the Natural Science Foundation of China (50632050, 20433060), the Program for New Century Excellent Talents in Universities of China (NCET-04-0688), and the National Hi-Tech R&D Program (2007AA05Z142), and made use of the facility in the Center for Electron Microscopy of Wuhan University.

**Supporting Information Available:** Experimental and computational details and supplemental figures. This material is available free of charge via the Internet at http://pubs.acs.org.

## References

(1) (a) Arenz, M.; Mayrhofer, K. J. J.; Stamenkovic, V.; Blizanac, B. B.; Tomoyuki, T.; Ross, P. N.; Markovic, N. M. *J. Am. Chem. Soc.* **2005**, *127*, 6819. (b) Mayrhofer, K. J. J.; Arenz, M.; Blizanac, B. B.; Stamenkovic, V.; Ross, P. N.; Markovic, N. M. *Electrochim. Acta* **2005**, *50*, 5144. (c) Maillard, F.; Savinova, E. R.; Simonov, P. A.; Zaikovskii, V. I.; Stimming, U. *J. Phys. Chem. B* **2004**, *108*, 17893. (d) Maillard, F.; Eikerling, M.; Cherstiouk, O. V.; Schreier, S.; Savinova, E.; Stimming, U. *Faraday Discuss.* **2004**, *125*, 357.

(2) (a) Bergamaski, K.; Pinheiro, A. L. N.; Teixeira-Neto, E.; Nart, F. C. *J. Phys. Chem. B* **2006**, *110*, 19271. (b) Mukerjee, S.; McBreen, J. *J. Electroanal. Chem.* **1998**, *448*, 163.

(3) (a) Yano, H.; Inukai, J.; Uchida, H.; Watanabe, M.; Babu, P. K.; Kobayashi, T.; Chung, J. H.; Oldfield, E.; Wieckowski, A. *Phys. Chem. Chem. Phys.* **2006**, *8*, 4932. (b) Mayrhofer, K. J. J.; Blizanac, B. B.; Arenz, M.; Stamenkovic, V. R.; Ross, P. N.; Markovic, N. M. *J. Phys. Chem. B* **2005**, *109*, 14433. (c) Maillard, F.; Martin, M.; Gloaguen, F.; Léger, J.-M. *Electrochim. Acta* **2002**, *47*, 3431. (d) Kinoshita, K. *J. Electrochem. Soc.* **1990**, *137*, 845.

(4) (a) Babić, B. M.; Vračar, L. M.; Radmilović, V.; Krstajić, N. V. *Electrochim. Acta* **2006**, *51*, 3820. (b) Takasu, Y.; Fujii, Y.; Yasuda, K.; Iwanaga, Y.; Matsuda, Y. *Electrochim. Acta* **1989**, *34*, 453. (c) Vogel, W.; Lundquist, J.; Ross, P.; Stonehart, P. *Electrochim. Acta* **1975**, *20*, 79.

(5) (a) Yang, B.; Lu, Q.; Wang, Y.; Zhuang, L.; Lu, J.; Liu, P.; Wang, J.; Wang, R. *Chem. Mater.* **2003**, *15*, 3552. (b) Zhao, D.; Feng, J.; Huo, Q.; Melosh, N.; Fredrickson, G. H.; Chmelka, B. F.; Stucky, G. D. *Science* **1998**, *279*, 548. (c) Jun, S.; Joo, S. H.; Ryoo, R.; Kruk, M.; Jaroniec, M.; Liu, Z.; Ohsuna, T.; Terasak, O. *J. Am. Chem. Soc.* **2000**, *122*, 10712.

(6) U. S. National Institute of Standards and Technology (NIST) XPS database, http://srdata.nist.gov/xps/.

(7) (a) Jacobsen, K. W.; Stoltze, P.; Nørskov, J. K. *Surf. Sci.* **1996**, *366*, 394. (b) Nielsen, L. P.; Besenbacher, F.; Stensgaard, I.; Lægsgaard, E.; Engdahl, C.; Stoltze, P.; Jacobsen, K. W.; Nørskov, J. K. *Phys. Rev. Lett.* **1993**, *71*, 754. (c) Nielsen, L. P.; Besenbacher, F.; Stensgaard, I.; Lægsgaard, E.; Engdahl, C.; Stoltze, P.; Nørskov, J. K. *Phys. Rev. Lett.* **1995**, *74*, 1159. (d) Christensen, A.; Ruban, A. V.; Stoltze, P.; Jacobsen, K. W.; Skriver, H. L.; Nørskov, J. K.; Besenbacher, F. *Phys. Rev. B* **1997**, *56*, 5822.

(8) Chen, S.; Kucernak, A. *J. Phys. Chem. B* **2004**, *108*, 13984.

(9) (a) Hammer, B. *Topics in Catal.* **2006**, *37*, 3. (b) Mavrikakis, M.; Hammer, B.; Nørskov, J. K. *Phys. Rev. Lett.* **1998**, *81*, 2819.

(10) Henry, C. R. *Surf. Sci. Rep.* **1998**, *31*, 231.

JA076177B